Title

Rad53 Downregulates Mitotic Gene Transcription by Inhibiting the Transcriptional Activator Ndd1

Journal

Molecular and Cellular Biology, 34(4)

ISSN

0270-7306

Authors

Edenberg, Ellen R
Vashisht, Ajay
Benanti, Jennifer A
et al.

Publication Date

2014-02-01

DOI

10.1128/mcb.01056-13

Peer reviewed

MCB
Journals.ASM.org

Rad53 Downregulates Mitotic Gene Transcription by Inhibiting the Transcriptional Activator Ndd1

Ellen R. Edenberg,[a] Ajay Vashisht,[b] Jennifer A. Benanti,[c] James Wohlschlegel,[b] David P. Toczyski[a]

Department of Biochemistry and Biophysics, University of California, San Francisco, San Francisco, California, USA[a]; Department of Biological Chemistry, University of California, Los Angeles, Los Angeles, California, USA[b]; Program in Gene Function and Expression, University of Massachusetts Medical School, Worcester, Massachusetts, USA[c]

The 33 genes in the *Saccharomyces cerevisiae* mitotic *CLB2* transcription cluster have been known to be downregulated by the DNA damage checkpoint for many years. Here, we show that this is mediated by the checkpoint kinase Rad53 and the dedicated transcriptional activator of the cluster, Ndd1. Ndd1 is phosphorylated in response to DNA damage, which blocks recruitment to promoters and leads to the transcriptional downregulation of the *CLB2* cluster. Finally, we show that downregulation of Ndd1 is an essential function of Rad53, as a hypomorphic *ndd1* allele rescues *RAD53* deletion.

Over a decade ago, a group of mitotic genes called the *CLB2* cluster was shown to be transcriptionally downregulated in response to DNA damage (1). The *CLB2* cluster consists of 33 coregulated mitotic genes, including those for its namesake, Clb2 (a B-type cyclin), Cdc5 (Polo kinase), Cdc20 (the activator of the anaphase promoting complex), Hst3 (a sirtuin histone deacetylase), and many others (3). Because so many important mitotic regulators are part of this cluster, it is a hub for the regulation of mitosis during the cell cycle and in response to DNA damage.

In an unperturbed cell cycle, *CLB2* cluster transcription is tightly regulated, with transcription off during G_1 phase and high in early mitosis (3–5). Throughout the cell cycle, Mcm1 and Fkh2 are present at the promoters of these mitotic genes and coordinate both repression and activation by recruiting additional transcriptional regulators (4, 5). During G_1, transcription of this cluster is off. As cells enter S phase, Clb5–cyclin-dependent kinase (CDK) phosphorylates Fkh2 (6). Later, Clb2-CDK and Cdc5 phosphorylate Ndd1, which leads to Ndd1's recruitment to its target promoters through an interaction with Fkh2 (7, 8, 27). Ndd1 then functions as a transcriptional activator to drive high levels of *CLB2* cluster transcription (4, 8). Ndd1 is itself cell cycle regulated and is transcribed in early S phase (9, 10). As both *CLB2* and *CDC5* are *CLB2* cluster members themselves, these phosphorylations generate a positive-feedback loop that drives switch-like transcription of the cluster. In addition, the precise timing of transcription of this cluster is modulated by protein kinase C (PKC) (11) and, for a subset of members, Yox1 (12, 13).

In response to DNA damage agents, transcription of the *CLB2* cluster is downregulated by the DNA damage checkpoint (1, 2). This checkpoint is a signal transduction cascade that is activated in response to genotoxic stress, and the checkpoint is required to prevent replication fork collapse and arrest the cell cycle (14, 15). At the top of the kinase cascade that makes up the checkpoint, the phosphatidylinositide 3-kinase-like kinase Mec1 (the homolog of human ATR) is activated. Mec1 then phosphorylates and activates downstream effector kinases Chk1 and Rad53 (homologs of human Chk1 and Chk2, respectively) (16). Chk1 has a well-described role in promoting cell cycle arrest by phosphorylating and thereby stabilizing Pds1 (the *Saccharomyces cerevisiae* securin) (17–19). Rad53 phosphorylates many downstream substrates, resulting in a block to late-origin firing, cell cycle arrest, and activation of the Dun1 kinase (20–24). Although prior work has examined the mechanism by which the DNA damage checkpoint promotes transcriptional induction of its target genes, the mechanisms of transcriptional inhibition are less well understood (25).

Here, we investigate the mechanism by which the DNA damage checkpoint controls the *CLB2* cluster. We find that Ndd1 is phosphorylated in a Rad53- and Dun1-dependent manner, which leads to the downregulation of the *CLB2* cluster and inhibits the recruitment of Ndd1 to Fkh2-bound promoters. Finally, we show that downregulation of Ndd1 is an essential function of *RAD53*.

MATERIALS AND METHODS

Yeast methods. Yeast strains were grown in YM-1 medium (28) with 2% dextrose at 30°C unless otherwise noted. Strains and plasmids were made using standard techniques. The *ndd1*^{m27} strain, a strain with 27 Rad53-dependent phosphorylation sites mutated, was purchased from DNA2.0. A detailed strain list is in Table 1; a detailed list of plasmids is in Table 2. For strains used in the experiments whose results are shown in Fig. 2 and 3, all strains except the *dun1*Δ strain were made by integrating a plasmid containing either the *NDD1* or *ndd1*^{m27} allele tagged with Flag into the genome as the sole copy. These were checked for single integration by Southern blotting.

For cell cycle experiments, cells were arrested with 10 μg/ml α-factor, 10 μg/ml nocodazole, 0.05% methyl methanesulfonate (MMS), or 0.2 M hydroxyurea for 2.5 to 3.5 h, as noted.

Cell cycle progression was followed by fixation of cells in 70% ethanol and storage of the cells at 4°C. Cells were sonicated and treated with 0.25 mg/ml RNase A for 1 h at 50°C, followed by digestion with 0.125 mg/ml proteinase K for 1 h at 50°C and labeling with 1 μM Sytox green. Data were collected using a FACSCalibur machine and analyzed with FlowJo software.

Received 16 August 2013 **Returned for modification** 7 September 2013
Accepted 4 December 2013
Published ahead of print 9 December 2013
Address correspondence to David P. Toczyski, toczyski@cc.ucsf.edu.
Supplemental material for this article may be found at http://dx.doi.org/10.1128/MCB.01056-13.

doi:10.1128/MCB.01056-13

TABLE 1 Strain list

Strain name	Strain background	Genotype	Figure, source
yERE87	S288C	*MAT***a** *his3Δ1 leu2Δ0 ura3Δ0* with pRSG1p-Ndd1	Fig. 1A, this study
yERE263	S288c	*MAT***a** *his3Δ1 leu2Δ0 ura3Δ0 lys2Δ0 sml1Δ::LEU2* with pEE38	Fig. 1B, this study
yERE251	S288c	*MAT***a** *his3Δ1 leu2Δ0 ura3Δ0 rad53Δ::KanMX sml1Δ::LEU2* with pEE38	Fig. 1B, this study
yERE241	S288C	*MAT***a** *his3Δ1 leu2Δ0 met15Δ0 ura3Δ0* with pRSG1-Ndd1	Fig. S1A in the supplemental material, this study
yERE242	S288C	*MAT***a** *his3Δ1 leu2Δ0 met15Δ0 ura3Δ0* with pRSG1-Ndd1-16A	Fig. S1A in the supplemental material, this study
yERE67	S288C	*MAT***a** *his3Δ1 leu2Δ0 met15Δ0 ura3Δ0 NDD1-URA3-GAL1*p-*NDD1*-3Flag-*HygMX*	Fig. 1C, this study
yERE72	S288C	*MAT***a** *his3Δ1 leu2Δ0 ura3Δ0 rad53Δ::KanMX sml1Δ::LEU2 NDD1-URA3-GAL1*p-*NDD1*-3Flag-*HygMX*	Fig. 1C, this study
yERE270	S288c	*MAT***a** *his3Δ1 leu2Δ0 ura3Δ0 lys2Δ0 sml1Δ::LEU2* with pEE39	Fig. 1D, this study
yERE258	S288c	*MAT***a** *his3Δ1 leu2Δ0 ura3Δ0 lys2Δ0 sml1Δ::LEU2 rad53::KanMX* with pEE39	Fig. 1D, this study
yERE268	S288c	*MAT***a** *his3Δ1 leu2Δ0 ura3Δ0 lys2Δ0 sml1Δ::LEU2* with pEE37	Fig. 1D, this study
yERE256	S288c	*MAT***a** *his3Δ1 leu2Δ0 ura3Δ0 lys2Δ0 sml1Δ::LEU2 rad53Δ::KanMX* with pEE37	Fig. 1D, this study
yERE430	S288c	*MAT***a** *his3Δ1 leu2Δ0 ura3Δ0 lys2Δ0* with pEE38	Fig. 1E, this study
yERE432	S288c	*MAT***a** *his3Δ1 leu2Δ0 ura3Δ0 lys2Δ0 dun1Δ::KanMX* with pEE38	Fig. 1E, this study
yERE107	S288C	*MAT***a** *his3Δ1 leu2Δ0 ura3Δ0 lys2Δ0 sml1Δ::LEU2 NDD1*p-*NDD1*-3Flag-*HygMX-URA3-ndd1Δ::HIS3*	Fig. 2 and 3 and Fig. S1B in the supplemental material, this study
yERE152	S288C	*MAT***a** *his3Δ1 leu2Δ0 ura3Δ0 lys2Δ0 sml1Δ::LEU2 NDD1*p-*NDD1*-3Flag-*HygMX-URA3-ndd1Δ*::HIS3	Fig. 2 and 3 and Fig. S2 in the supplemental material, this study
yERE108	S288C	*MAT***a** *his3Δ1 leu2Δ0 ura3Δ0 lys2Δ0 sml1Δ::LEU2 rad53Δ::KanMX NDD1*p-*NDD1*-3Flag-*HygMX-URA3-ndd1Δ::HIS3*	Fig. 2 and 3 and Fig. S1B in the supplemental material, this study
yERE153	S288C	*MAT***a** *his3Δ1 leu2Δ0 ura3Δ0 lys2Δ0 sml1Δ::LEU2 rad53Δ::KanMX NDD1*p-*NDD1*-3Flag-*HygMX-URA3-ndd1Δ::HIS3*	Fig. 2 and 3 and Fig. S2 in the supplemental material, this study
yERE109	S288C	*MAT***a** *his3Δ1 leu2Δ0 ura3Δ0 lys2Δ0 sml1Δ::LEU2 NDD1*p-*ndd1*^{m27}-3Flag-*HygMX-URA3-ndd1Δ::HIS3*	Fig. 2 and 3 and Fig. S1B in the supplemental material, this study
yERE151	S288C	*MAT***a** *his3Δ1 leu2Δ0 ura3Δ0 lys2Δ0 sml1Δ::LEU2 NDD1*p-*ndd1*^{m27}-3Flag-*HygMX-URA3-ndd1Δ::HIS3*	Fig. 2 and 3 and Fig. S2 in the supplemental material, this study
yERE111	S288C	*MAT***a** *his3Δ1 leu2Δ0 ura3Δ0 lys2Δ0 sml1Δ::LEU2 rad53Δ::KanMX NDD1*p-*ndd1*^{m27}-3Flag-*HygMX-URA3-ndd1Δ::HIS3*	Fig. 2 and 3 and Fig. S1B in the supplemental material, this study
yERE149	S288C	*MAT***a** *his3Δ1 leu2Δ0 ura3Δ0 lys2Δ0 sml1Δ::LEU2 rad53Δ::KanMX NDD1*p-*ndd1*^{m27}-3Flag-*HygMX-URA3-ndd1Δ::HIS3*	Fig. 2 and 3 and Fig. S2 in the supplemental material, this study
dun1Δ	S288C	*MAT***a** *his3Δ1 leu2Δ0 met15Δ0 ura3Δ0 dun1Δ::KanMX*	Fig. 2, yeast knockout collection
yERE145	S288C	*MAT***a** *his3Δ1 leu2Δ0 ura3Δ0 lys2Δ0 sml1Δ::LEU2 NDD1*p-*NDD1*^{10A}-3Flag-*HygMX-URA3-ndd1Δ::HIS3*	Fig. 2C and 3A, this study
yERE146	S288C	*MAT***a** *his3Δ1 leu2Δ0 ura3Δ0 lys2Δ0 sml1Δ::LEU2 rad53Δ::KanMX NDD1*p-*NDD1*^{10A}-3Flag-*HygMX-URA3-ndd1Δ::HIS3*	Fig. 2C and 3A, this study
yERE147	S288C	*MAT***a** *his3Δ1 leu2Δ0 ura3Δ0 lys2Δ0 sml1Δ::LEU2 NDD1*p-*ndd1*^{m17}-3Flag-*HygMX-URA3-ndd1Δ::HIS3*	Fig. 2C and 3A, this study
yERE148	S288C	*MAT***a** *his3Δ1 leu2Δ0 ura3Δ0 lys2Δ0 sml1Δ::LEU2 rad53Δ::KanMX NDD1*p-*ndd1*^{m17}-3Flag-*HygMX-URA3-ndd1Δ::HIS3*	Fig. 2C and 3A, this study
yERE156	S288C	*MAT***a** *his3Δ1 leu2Δ0 ura3Δ0 lys2Δ0 sml1Δ::LEU2 NDD1*p-*ndd1*^{25A}-3Flag-*HygMX-URA3-ndd1Δ::HIS3*	Fig. 2C and 3A, this study
yERE157	S288C	*MAT***a** *his3Δ1 leu2Δ0 ura3Δ0 lys2Δ0 sml1Δ::LEU2 rad53Δ::KanMX NDD1*p-*ndd1*^{25A}-3Flag-*HygMX-URA3-ndd1Δ::HIS3*	Fig. 2C and 3A, this study
MW83-6A	S288C	*MAT***a** *his3Δ1 leu2Δ0 met15Δ0 ura3Δ0*	Fig. 4A and E, C. Boone
yERE40	S288C	*MAT***a** *his3Δ1 leu2Δ0 met15Δ0 ura3Δ0 FKH2*-3Flag-*HygMX*	Fig. 4A and B, this study
yERE41	S288C	*MAT***a** *his3Δ1 leu2Δ0 met15Δ0 ura3Δ0 NDD1*-3Flag-*HygMX*	Fig. 4C and F, this study
yERE48	S288C	*MAT***a** *his3Δ1 leu2Δ0 ura3Δ0 rad53Δ::KanMX sml1Δ::LEU2 NDD1*-3Flag-*HygMX*	Fig. 4C and D, this study
yERE439	S288C	*MAT***a** *his3Δ1 leu2Δ0 met15Δ0 ura3Δ0 NDD1*-3Flag-*HygMX*	Fig. 4E and F, this study (same as yERE41)
yERE440	S288C	*MAT***a** *his3Δ1 leu2Δ0 ura3Δ0 dun1Δ::KanMX NDD1*-3Flag-*HygMX*	Fig. 4E and F, this study
yERE456	S288C	*MAT***a** *his3Δ1 leu2Δ0 ura3Δ0 trp1Δ::KanMX sml1Δ::LEU2 gal4Δ::HIS3 gal80Δ::URA3* with pEE20	Fig. 4G and 5B and Fig. S3 and S4 in the supplemental material, this study
yERE457	S288C	*MAT***a** *his3Δ1 leu2Δ0 ura3Δ0 trp1Δ::KanMX sml1Δ::LEU2 gal4Δ::HIS3 gal80Δ::URA3* Nat^{r}-*ADH1*p-Ndd1^{wt}-Flag-HYG with pEE20	Fig. 4G and 5B and Fig. S3 and S4 in the supplemental material, this study

(Continued on following page)

TABLE 1 (Continued)

Strain name	Strain background	Genotype	Figure, source
yERE458	S288C	*MAT***a** *his3*Δ*1 leu2*Δ*0 ura3*Δ*0 trp1*Δ::*KanMX sml1*Δ::*LEU2 rad53*Δ::*KanMX gal4*Δ::*HIS3 gal80*Δ::*URA3* Nat^r-*ADH1*p-Ndd1^{wt}-Flag-HYG with pEE20	Fig. 4G and 5B and Fig. S3 and S4 in the supplemental material, this study
yERE459	S288C	*MAT***a** *his3*Δ*1 leu2*Δ*0 ura3*Δ*0 trp1*Δ::*KanMX sml1*Δ::*LEU2 gal4*Δ::*HIS3 gal80*Δ::*URA3* Nat^r-*ADH1*p-Ndd1^{m27}-Flag-HYG with pEE20	Fig. 4G and 5B and Fig. S3 and S4 in the supplemental material, this study
yERE460	S288C	*MAT***a** *his3*Δ*1 leu2*Δ*0 ura3*Δ*0 trp1*Δ::*KanMX sml1*Δ::*LEU2 gal4*Δ::*HIS3 gal80*Δ::*URA3* Nat^r-*ADH1*p-Ndd1^{m27}-Flag-HYG with pEE20	Fig. 4G and 5B and Fig. S3 and S4 in the supplemental material, this study
yERE336	S288C	*MAT***a** *his3*Δ*1 leu2*Δ*0 ura3*Δ*0 trp1*Δ::*KanMX sml1*Δ::*LEU2 gal4*Δ::*HIS3 gal80*Δ::*URA3* Nat^r-*ADH1*p-Ndd1 with pEE20	Fig. 5A, this study
yERE337	S288C	*MAT***a** *his3*Δ*1 leu2*Δ*0 ura3*Δ*0 trp1*Δ::*KanMX sml1*Δ::*LEU2 rad53*Δ::*KanMX gal4*Δ::*HIS3 gal80*Δ::*URA3* Nat^r-*ADH1*p-Ndd1 with pEE20	Fig. 5A, this study
yERE338	S288C	*MAT***a** *his3*Δ*1 leu2*Δ*0 ura3*Δ*0 trp1*Δ::*KanMX sml1*Δ::*LEU2 gal4*Δ::*HIS3 gal80*Δ::*URA3* Nat^r-*ADH1*p-Ndd1 with pGBKT7	Fig. 5A, this study
yERE300	S288C	*MAT***a** *his3*Δ*1 leu2*Δ*0 ura3*Δ*0 trp1*Δ::*KanMX sml1*Δ::*LEU2 gal4*Δ::*HIS3 gal80*Δ::*URA3* with pAS1796	Fig. 5C, this study
yERE301	S288C	*MAT***a** *his3*Δ*1 leu2*Δ*0 ura3*Δ*0 trp1*Δ::*KanMX sml1*Δ::*LEU2 rad53*Δ::*KanMX gal4*Δ::*HIS3 gal80*Δ::*URA3* with pAS1796	Fig. 5C, this study
yERE304	S288C	*MAT***a** *his3*Δ*1 leu2*Δ*0 ura3*Δ*0 trp1*Δ::*KanMX sml1*Δ::*LEU2 gal4*Δ::*HIS3 gal80*Δ::*URA3* with pGBKT7	Fig. 5C, this study
yERE305	S288C	*MAT***a** *his3*Δ*1 leu2*Δ*0 ura3*Δ*0 trp1*Δ::*KanMX sml1*Δ::*LEU2 rad53*Δ::*KanMx gal4*Δ::*HIS3 gal80*Δ::*URA3* with pGBKT7	Fig. 5C, this study
yERE307	LS	*MAT*Δ *trp1 his3 ura3 leu2 can1 lys5 ade2 cyh2 ade3*::*GAL1*p-HO *NDD1^{wt}*-3Flag-Hyg with extra chromosome VII [*aro2 tel1*::*URA3*]	Fig. 6A and B, this study
yERE308	LS	*MAT*Δ *trp1 his3 ura3 leu2 can1 lys5 ade2 cyh2 ade3*::*GAL1*p-HO *ndd1^{m27}*-3Flag-Hyg with extra chromosome VII [*aro2 tel1*::*URA3*]	Fig. 6A and B, this study
yERE462	LS	*MAT*Δ *trp1 his3 ura3 leu2 can1 lys5 ade2 cyh2 ade3*::*GAL1*p-HO *ndd1^{m27}*-3Flag-Hyg-*HIS-NDD1^{wt}*-3Flag-Hyg with extra chromosome VII [*aro2 tel1*::*URA3*]	Fig. S5A in the supplemental material, this study
yERE463	LS	*MAT*Δ *trp1 his3 ura3 leu2 can1 lys5 ade2 cyh2 ade3*::*GAL1*p-HO *ndd1^{m17}*-3Flag-Hyg-HIS-*NDD1^{wt}*-3Flag-Hyg with extra chromosome VII [*aro2 tel1*::*URA3*]	Fig. S5A in the supplemental material, this study
yERE464	LS	*MAT*Δ *trp1 his3 ura3 leu2 can1 lys5 ade2 cyh2 ade3*::*GAL1*p-HO *ndd1^{25A}*-3Flag-Hyg-*HIS-NDD1^{wt}*-3Flag-Hyg with extra chromosome VII [*aro2 tel1*::*URA3*]	Fig. S5A in the supplemental material, this study
yERE405	S288c	*MAT***a**/α *his3*Δ*1/his3*Δ*1 leu2*Δ*0/leu2*Δ*0 met15*Δ*0/MET15 ura3*Δ*0/ura3*Δ*0 lys2*Δ*0/LYS2 rad53*Δ::*URA3/RAD53 ndd1^{hyp}*-3Flag-*HygMX-URA3-ndd1*Δ::*HIS3/NDD1*	Fig. 6C, this study
yERE451	S288c	*his3*Δ*1 leu2*Δ*0 ura3*Δ*0 RAD53 NDD1 sml1*Δ::*LEU2*	Fig. S5B in the supplemental material, this study
yERE452	S288c	*his3*Δ*1 leu2*Δ*0 ura3*Δ*0 RAD53 ndd1^{hyp}*-3Flag-*HygMX-URA3-ndd1*Δ::*HIS3 sml1*Δ::*LEU2*	Fig. S5B in the supplemental material, this study
yERE453	S288c	*his3*Δ*1 leu2*Δ*0 ura3*Δ*0 rad53*Δ::*URA3 NDD1 sml1*Δ::*LEU2*	Fig. S5B in the supplemental material, this study
yERE454	S288c	*his3*Δ*1 leu2*Δ*0 ura3*Δ*0 rad53*Δ::*URA3 ndd1^{hyp}*-3Flag-*HygMX-URA3-ndd1*Δ::*HIS3 sml1*Δ::*LEU2*	Fig. S5B in the supplemental material, this study

Western blotting. Cell pellets of equivalent optical densities (ODs) were collected, washed with 1 ml 4°C H_2O, and frozen on dry ice. Pellets were thawed in boiling sample buffer (50 mM Tris, pH 7.5, 5% SDS, 5 mM EDTA, 10% glycerol, 0.5% β-mercaptoethanol, bromophenol blue, 1 μg/ml leupeptin, 1 μg/ml bestatin, 0.1 mM benzamidine, 1 μg/ml pepstatin A, 5 mM NaF, 1 mM Na_3VO_4, 80 mM β-glycerophosphate, 1 mM phenylmethylsulfonyl fluoride). Cells were boiled for 3 min, beaten with glass beads for 3 min, and clarified by centrifugation. Extracts were analyzed by SDS-PAGE and Western blotting. Western blot analyses were performed with low-salt phosphate-buffered saline with Tween 20 (PBS-T) (15 mM NaCl, 1.3 mM NaH_2PO_4, 5.4 mM Na_2HPO_4, 0.05% Tween 20). Primary antibody incubations were performed in 5% nonfat dry milk and low-salt PBS-T. Antibodies were used as follows: anti-Flag (clone M2; Sigma-Aldrich) at 1:2,000, antihemagglutinin (anti-HA; HA.11; Covance) at 1:1,000, and anti-Rad53 (DAB001; a gift from the lab of D. Durocher) at 1:2,000.

Mass spectrometry analysis. *GAL1*p-Ndd1-Flag was induced in YM-1 medium with 2% galactose. Wild-type and *rad53*Δ strains were grown to an OD of approximately 0.4 and then treated with 0.05% MMS for 3 h. Two liters of cells was collected for each sample. Pellets were lysed in lysis buffer (25 mM HEPES, pH 7.5, 250 mM NaCl, 0.2% Triton X-100, 1 mM EDTA, 10% glycerol, 1 μg/ml leupeptin, 1 μg/ml bestatin, 0.1 mM benzamidine, 1 μg/ml pepstatin A, 5 mM NaF, 1 mM Na_3VO_4, 80 mM β-glycerophosphate, 1 mM phenylmethylsulfonyl fluoride) by beating with glass beads 5 to 7 times for 1.5-min intervals in a cold block, with the cells rested on ice between intervals. Samples were clarified by centrifuga-

TABLE 2 Plasmid list

Plasmid name	Description	Figure (source or reference)
pRSG1p-Ndd1	HIS marked CEN/ARS plasmid with *GAL1*p-Ndd1-3HA	Fig. 1A and Fig. S1A in the supplemental material (this study)
pRSG1p-Ndd1-16A	HIS marked CEN/ARS plasmid with *GAL1*p-Ndd1$^{cdk\Delta}$-3HA	Fig. S1A in the supplemental material (this study)
pEE38	pRS316 with *NDD1*p-Ndd1$^{cdk\Delta}$-3Flag-HYG^r	Fig. 1B and E (this study)
pEE39	pRS316 with *NDD1*p-Ndd1$^{cdk\Delta}$-3Flag-HYG^r	Fig. 1D (identical to pEE38) (this study)
pEE37	pRS316 with *NDD1*p-Ndd1$^{cdk\Delta\text{-}m27}$-3Flag-HYG^r	Fig. 1D (this study)
pGBKT7	*ADH1*p-Gal4$_{DBD}$ alone	Fig. 5A and B
pEE20	pGBKT7 with *ADH1*p-Gal4$_{DBD}$-Fkh2	Fig. 5A (this study)
pAS1796	pGBKT7 with *ADH1*p-Gal4$_{DBD}$-Ndd1	Fig. 5B (8)

tion. Purification was done by immunoprecipitation with anti-Flag antibody (clone M2) for 3 to 5 h with rotation at 4°C. Beads were washed 6 times with lysis buffer supplemented to 500 mM NaCl. Purified protein was eluted with 150 μg/ml 3-Flag peptide. Samples were concentrated by trichloroacetic acid precipitation and run on SDS-polyacrylamide gels, and the band corresponding to Ndd1 was cut out and sent for mass spectrometry analysis.

Mass spectrometry analysis was done as described previously (20). We also found 9 additional sites of lower confidence that we did not include in our analysis (S13, T126, S197, T253, S260, S356, T360, T368, and S416).

ChIP. Chromatin immunoprecipitation (ChIP) was performed essentially as described in reference 26, with the following changes. Briefly, cells were cross-linked with 1.08% formaldehyde for 10 min and then quenched with 140 mM glycine for 10 min. Cells were lysed by bead beating in lysis buffer (50 mM HEPES, pH 7.5, 140 mM NaCl, 1 mM EDTA, 1% Triton X-100, 0.1% Na deoxycholate, 1 μg/ml leupeptin, 1 μg/ml bestatin, 0.1 mM benzamidine, 1 μg/ml pepstatin A, 5 mM NaF, 1 mM Na_3VO_4, 80 mM β-glycerophosphate, 1 mM phenylmethylsulfonyl fluoride), and DNA was fragmented by sonication. The supernatant was incubated with anti-Flag antibody (clone M2) on magnetic beads for at least 3 h. Coprecipitated DNA was analyzed by PCR and run on an agarose gel. Quantification of ChIP data was done by quantitative PCR (qPCR) using 0.5 μl to 1 μl of purified DNA in a 20-μl reaction mixture with SsoFast EvaGreen Supermix (Bio-Rad) on a Stratagene Mx3000p qPCR system. Relative copy number was calculated on the basis of a standard curve generated in each experiment from genomic DNA using the same primer set. To quantify the ChIP data, each immunoprecipitate (IP) sample was normalized to the corresponding whole-cell extract (WCE) input sample. To compare between experiments, the IP/WCE ratios were then normalized by setting the highest IP/WCE ratio within the experiment equal to 1. For all ChIP experiments with Ndd1 under the control of the *ADH1* promoter (experiments whose results are shown in Fig. 4G and 5B and Fig. S3 and S4 in the supplemental material), the strains contained the Gal4 DNA-binding domain (Gal4$_{DBD}$)–Fkh2 fusion-carrying plasmid pEE20. For these experiments, cells were grown and arrested in α-factor while selecting for the plasmid (in synthetic medium without tryptophan) and then released into YM-1 medium with 2% dextrose.

RNA purification and RT-qPCR. Cell pellets were collected, washed with 1 ml of cold H_2O, and frozen on dry ice. RNA was purified using a Qiagen RNeasy kit with bead beating. DNase treatment was done using a DNA-free RNA kit from Zymo Research. Reverse transcription (RT) was done using random primers and SuperScript III reverse transcriptase (Invitrogen), followed by digestion with RNase H (NEB). For qPCR, 1 μl cDNA was added to a 20-μl reaction mixture with SsoFast EvaGreen Supermix (Bio-Rad). For each sample, a control lacking reverse transcriptase was included, and the value for any product resulting from genomic DNA contamination was subtracted from the final values. qPCRs were carried out on a Stratagene Mx3000P qPCR system. Relative copy number was calculated on the basis of a standard curve generated in each experiment from genomic DNA using the same primer set. mRNA levels for each sample were calculated by first subtracting any signal from the no-reverse-transcriptase control and then normalizing to the corresponding *ACT1* value. To calculate the fold repression, the level of mitotic transcription from 45 min after release from G_1 was divided by the level of damaged transcription from 90 min after release from G_1 into 0.05% MMS. For the experiments whose results are shown in Fig. 5A, we found that with Ndd1 under the control of its endogenous promoter, transcription driven by Gal4$_{DBD}$-Fkh2 was at background levels. Therefore, we overexpressed Ndd1 under the control of the *ADH1* promoter in these strains.

Chromosome loss assay. *ade2 ade3* strains harboring an extra chromosome VII (which contains *CYH2* and *ADE3*) were grown at 23°C on synthetic medium lacking lysine and tyrosine to select for both copies of chromosome VII. Cells were grown overnight before plating onto rich medium (yeast extract-peptone-dextrose [YPD]) for visualization of chromosome loss by the appearance of white sectors in otherwise red colonies. Cells were also plated onto rich medium containing 10 μg/ml cycloheximide to score white, cycloheximide-resistant colonies for quantification. While most cycloheximide-resistant colonies had lost the extra chromosome VII containing *CYH2*, some may have mutated that gene, and these were still included in our count. For the gain-of-function chromosome loss experiments whose results are shown in Fig. S5A in the supplemental material, the second mutant *NDD1* allele was integrated at the endogenous *NDD1* locus.

***rad53*Δ strain viability rescue and sensitivity experiment.** The *ndd1* hypomorphic allele (*ndd1^{hyp}*) was made by mutating 5 CDK sites on *NDD1* to alanine (S254A, T265A, T277A, S409A, and T411A) and was integrated at the endogenous *NDD1* locus over a deletion of the endogenous *NDD1*. A diploid strain heterozygous for *ndd1^{hyp}* and *rad53*Δ was sporulated, and tetrads were dissected. Plates were incubated for 6 days before being photographed.

For the sensitivity experiment whose results are shown in Fig. S5B in the supplemental material, cells dissected from a diploid strain heterozygous for *ndd1^{hyp}*, *rad53*Δ, and *sml1*Δ were sporulated to generate all relevant genotypes. Cells were grown overnight, diluted to the same OD, and then spotted onto YPD plates or YPD plates with 0.005% MMS.

RESULTS

Ndd1 is a target of the DNA damage checkpoint. In order to understand how the *CLB2* cluster is downregulated in response to DNA damage (1, 2), we investigated whether the known transcriptional activator of the *CLB2* cluster, Ndd1, was modified. Ndd1 shifted in cells treated with the DNA-damaging agent MMS (Fig. 1A). However, in cells arrested in metaphase by treatment with nocodazole, Ndd1 also had a characteristic phosphoshift consistent with its known activating phosphorylations by CDK and Cdc5 (7, 8, 27). To eliminate the confounding effects of Ndd1 phosphorylation by these cell cycle kinases, we generated an allele of Ndd1 that eliminated these phosphorylation sites, changing all 16 minimal CDK consensus sites (serine or threonine followed by a proline [S/T-P]) to alanine to create an Ndd1 allele that cannot be modified by CDK (Ndd1$^{cdk\Delta}$). Since CDK phosphorylation is required for the essential function of *NDD1* (27), we examined

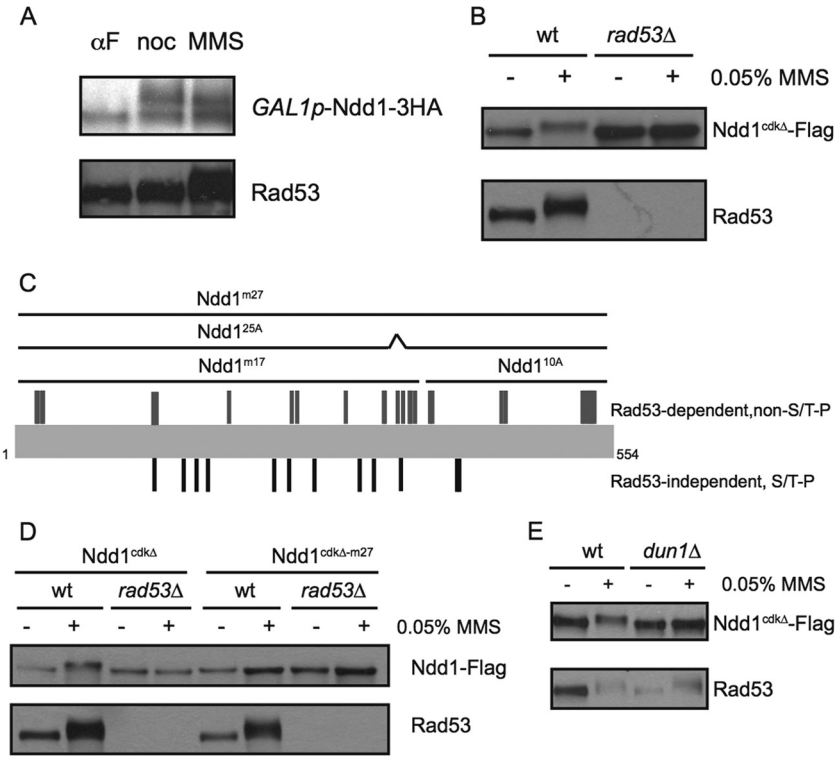

FIG 1 Ndd1 is a target of the DNA damage checkpoint. (A) Cells expressing Ndd1-3HA from the *GAL1* promoter (*GAL1*p-Ndd1-3HA) were arrested in α-factor (αF), nocodazole (noc), or 0.05% MMS for 3.5 h. Whole-cell extracts were blotted and probed for Ndd1-HA or Rad53. (B) Cells expressing Ndd1$^{cdk\Delta}$-Flag from its endogenous promoter were collected 60 min after release from α-factor into the absence (−) or presence (+) of 0.05% MMS to compare cells in an unperturbed mitosis to those that have been damaged. Samples were processed as described for panel A. (C) Phosphorylation sites on Ndd1 were mapped by mass spectrometry. *GAL1*p-Ndd1-Flag was induced and purified from wild-type or *rad53*Δ strains after 3 h in the presence of 0.05% MMS. Twenty-seven Rad53-dependent (non-S/T-P) sites are shown above the gray bar. Rad53-independent phosphorylation sites and S/T-P sites are shown beneath the gray bar and include 11 of the 16 CDK consensus sites. Subsets mutated for different Ndd1 mutants are denoted above. (D) Cells expressing Ndd1$^{cdk\Delta}$-Flag or Ndd1$^{cdk\Delta\text{-}m27}$-Flag (additionally mutating the Rad53-dependent, non-S/T-P phosphorylation sites shown in panel C) were collected 60 min after release from α-factor in the absence (−) or presence (+) of 0.05% MMS and processed as described for panel A. (E) Experiment done as described for panel B from wild-type and *dun1*Δ strains.

this allele, tagged with the Flag epitope, in the context of untagged wild-type *NDD1*. Ndd1$^{cdk\Delta}$ no longer shifted in an undamaged mitosis (see Fig. S1A in the supplemental material) but still shifted in response to DNA damage in a Rad53-dependent manner (Fig. 1B). This suggested that Ndd1 is phosphorylated by the DNA damage checkpoint, independently of its known phosphorylation regulation during an unperturbed cell cycle. Moreover, since CDK phosphorylation of Ndd1 is required for Ndd1 to be recruited to promoters (27) by its binding partner Fkh2 (8), Ndd1 targeting by Rad53 must be independent of its recruitment.

We used mass spectrometry to map Rad53-dependent phosphorylation sites on Ndd1. Ndd1 was overexpressed and purified from wild-type or *rad53*Δ cells in the presence of MMS. We found that Ndd1 was very heavily phosphorylated (Fig. 1C; details are provided in Table S1 in the supplemental material), and we identified 11 of the 16 potential CDK sites (S/T-P) in at least one of our purifications. We also identified 27 additional Rad53-dependent phosphorylation sites on Ndd1. Mutation of these 27 phosphorylation sites in the context of the Ndd1$^{cdk\Delta}$ allele (Ndd1$^{cdk\Delta\text{-}m27}$) and wild-type Ndd1 (Ndd1^{m27}) no longer showed a Rad53-dependent phosphorylation shift in response to DNA damage (Fig. 1D; see Fig. S1B in the supplemental material). One of Rad53's many downstream substrates is another checkpoint kinase, Dun1 (22). We found that the Ndd1$^{cdk\Delta}$ shift in response to DNA damage was also Dun1 dependent (Fig. 1E).

Ndd1^{m27} is resistant to Rad53-dependent downregulation of *CLB2* cluster transcription. We wanted to test whether Ndd1 regulation by Rad53 and Dun1 was responsible for *CLB2* cluster transcriptional downregulation in response to DNA damage. To measure *CLB2* cluster transcription, we arrested cells in G_1 and released them into the absence or presence of MMS. We followed transcription of *HST3*, one member of the *CLB2* cluster, after release from G_1 (Fig. 2A), normalizing transcription to the levels seen in G_1-arrested cells. We found that *HST3* transcription was induced almost 15-fold in a normal mitosis, peaking 45 min after release from G_1, and was significantly reduced in response to DNA damage, even 90 min after release from G_1 ($P < 0.0001$ by one-tailed Student *t* test), although the level of transcription in the presence of DNA damage was still 5-fold higher than that in the actively repressed G_1-arrested cells (Fig. 2Ai). Downregulation of *HST3* transcription in response to DNA damage requires Rad53, as the *rad53*Δ strain showed even higher levels of transcription in response to damage compared to that in an unperturbed mitosis (Fig. 2Aii), consistent with previous reports that transcriptional downregulation of the *CLB2* cluster requires the upstream DNA damage checkpoint kinase Mec1 (1, 2), which is required for Rad53 activity. However, even in a *rad53*Δ strain, *HST3* transcription was delayed in MMS and was still rising between 60 and 90 min after release from G_1 (compared to the transcriptional peak at 45 min in an unperturbed mitosis). This is presumably due to the

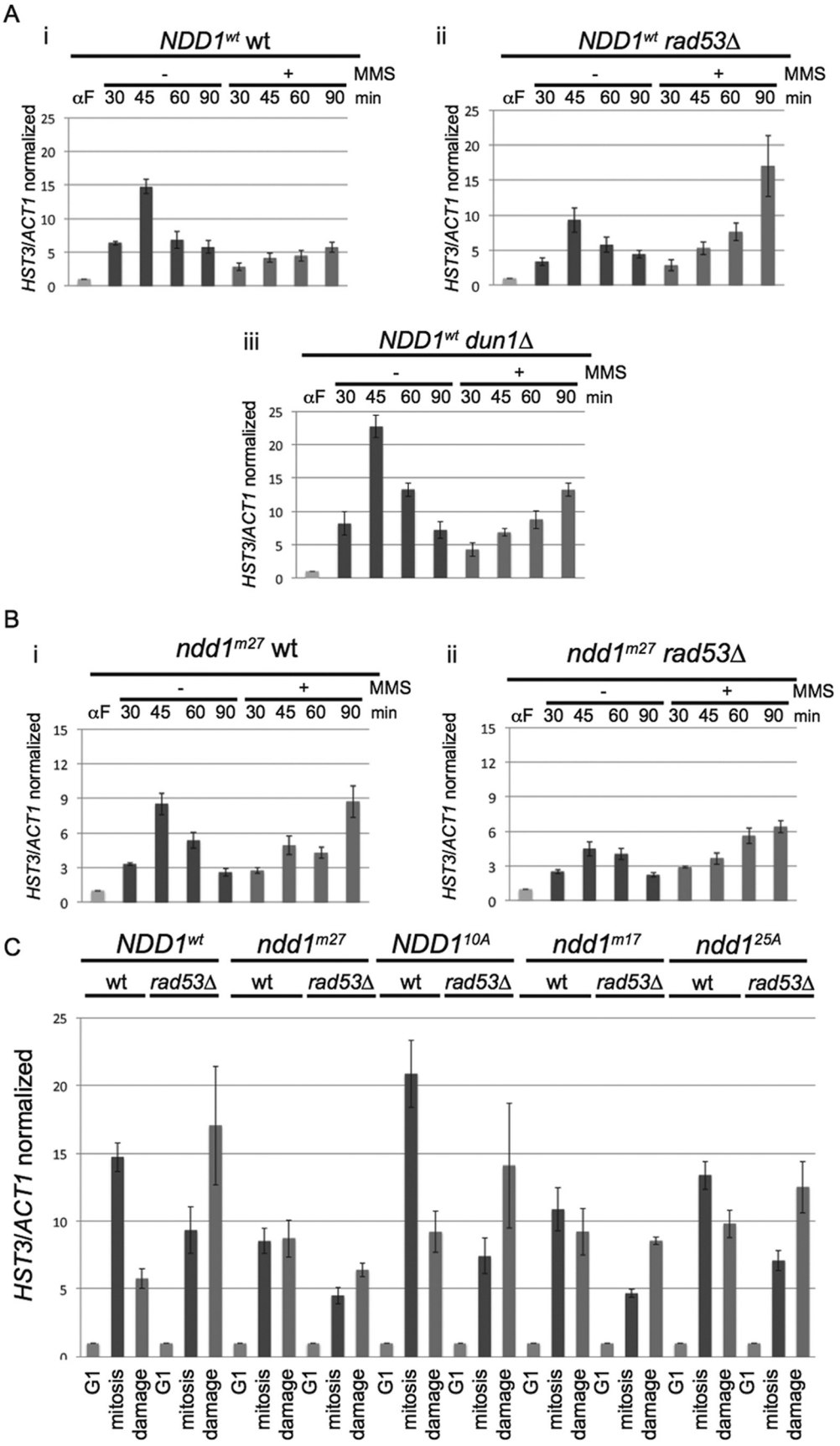
A
i
NDD1wt wt
ii
NDD1wt rad53Δ
iii
NDD1wt dun1Δ
MMS
αF 30 45 60 90 30 45 60 90 min
HST3/ACT1 normalized
B
i
ndd1m27 wt
ii
ndd1m27 rad53Δ
C
NDD1wt
ndd1m27
NDD110A
ndd1m17
ndd125A
wt
rad53Δ
G1
mitosis
damage

alkylation of the genome by MMS and the slowing of the cell cycle independently of the checkpoint (fluorescence-activated cell sorter data for cell cycle progression of wild-type and *rad53*Δ cells are shown in Fig. S2A in the supplemental material, and comparison of cell cycle progression 45 min after release from G_1 in *rad53*Δ cells is shown in Fig. S2B in the supplemental material). We found that Dun1 had a partial effect on the transcriptional repression of *HST3* (Fig. 2Aiii). Transcription in response to DNA damage was still repressed in *dun1*Δ cells ($P < 0.001$ by one-tailed Student *t* test), but unlike the 3-fold repression seen in wild-type cells, transcription was repressed only 1.8-fold in this mutant (comparing maximal transcription from an undamaged mitosis to maximal transcription in response to damage, $P = 0.023$ by one-tailed Student *t* test).

To test whether the phosphorylation of Ndd1 was responsible for the downregulation of mitotic gene transcription, we generated an *ndd1*^{m27} mutant, which lacks all of the mapped Rad53-dependent phosphorylation sites. Although the *ndd1*^{m27} mutant is slightly hypomorphic (compare the undamaged transcription in Fig. 2Ai and Bi), the *ndd1*^{m27} mutant is functional, as *NDD1* is essential, and *ndd1*^{m27} mutants showed no fitness or cell cycle defect (see Fig. S2C in the supplemental material). Unlike *NDD1* cells, *ndd1*^{m27} mutants showed similar levels of *HST3* transcription in the presence and absence of DNA damage (comparing the mitotic transcriptional peak at 45 min to damage transcription after 90 min) (Fig. 2Bi), and *rad53*Δ was epistatic to *ndd1*^{m27} (Fig. 2Bii), suggesting that Ndd1 is the primary Rad53 target responsible for downregulating transcription of the *CLB2* cluster in response to DNA damage. The loss of transcriptional repression of *HST3* in response to damage was stronger in the *ndd1*^{m27} mutant than in the *dun1*Δ mutant, leading us to the conclusion that Ndd1 is phosphorylated by both Rad53 and Dun1. Since Rad53 is required for the activation of Dun1, we used a *rad53*Δ mutant for the rest of our analysis to eliminate the contribution of both kinases.

We wanted to know whether a specific subset of our identified sites was responsible for the downregulation of *HST3* transcription in the presence of DNA damage (Fig. 2C). We tested three additional mutants. The *NDD1*^{10A} mutant has the last 10 sites mutated, while the *ndd1*^{m17} mutant has the first 17 sites mutated. The *ndd1*^{25A} mutant has all sites mutated except for two (Y354 and T359) that fall very close to the predicted Polo box binding site. For all mutants, we compared mitotic transcription (from 45 min after release from G_1) to damaged transcription (from 90 min after release from G_1 into MMS). For the *ndd1*^{m17} and *ndd1*^{25A} mutants, the level of *HST3* transcription in response to damage was very close to that seen in the absence of damage, but both mutants were slightly hypomorphic (comparing the mitotic transcription level to that for the wild-type *NDD1* [*NDD1*^{wt}] strain).

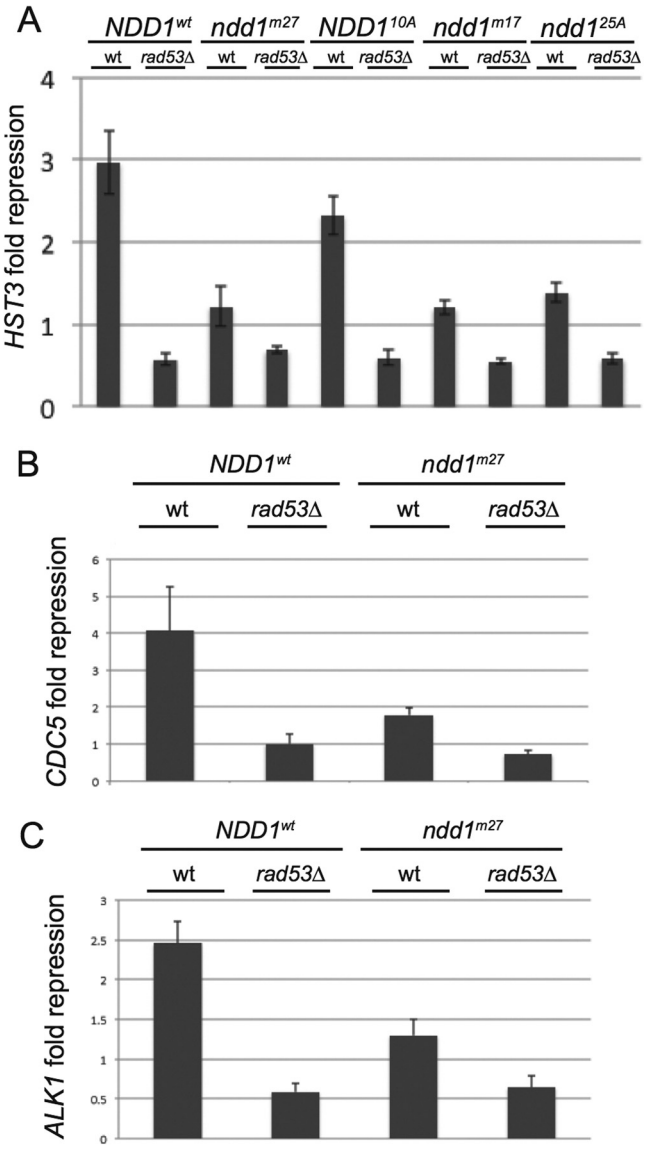

FIG 3 Ndd1 phosphorylation leads to downregulation of mitotic genes. (A) Alternative representation of the data in Fig. 2. Fold repression is calculated as the ratio of mitotic transcription (45 min after release from G_1) to damaged transcription (90 min after release from G_1). A value of 1 reflects no difference. Error bars reflect SEMs from 3 or more independent biological replicates. (B and C) As described for panel A, except that *CLB2* cluster members *CDC5* and *ALK1* were examined. Data are presented as the means ± SEMs from 4 or more independent biological replicates.

FIG 2 Rad53-dependent phosphorylation of Ndd1 leads to the downregulation of mitotic gene transcription in response to DNA damage. (A and B) For all panels, cells were arrested in G_1 with α-factor and released into the absence (−) or presence (+) of 0.05% MMS for the indicated times. Transcription was measured by RT-qPCR analysis. *HST3* transcript levels were normalized to *ACT1* levels; values were then normalized to *HST3* levels in G_1 for each strain. Error bars reflect SEMs from 3 or more independent biological replicates. The wild-type (Ai and Bi) and *rad53*Δ (Aii and Bii) strains are also *sml1*Δ and Ndd1-Flag or Ndd1^{m27}-Flag. (C) Cells were arrested in G_1 with α-factor and released into the absence of MMS for 45 min (mitosis) or the presence of 0.05% MMS for 90 min (damage). Transcription was measured by RT-qPCR analysis. *HST3* transcript levels were normalized to *ACT1* levels; values were then normalized to *HST3* levels in G_1 for each strain, as described for panels A and B. Data for *NDD1*^{wt} and *NDD1*^{m27} are the same as in panels A and B. As shown in Fig. 1C, *NDD1*^{10A} is mutated for the C-terminal 10 Rad53-dependent sites identified (from S384 to the end). *NDD1*^{m17} has the N-terminal 17 Rad53-dependent sites mutated (up to S370). *NDD1*^{25A} has all Rad53-dependent sites mutated, except for Y354 and T359, which fall very close to the predicted Polo box binding site. All strains are *sml1*Δ and Ndd1-Flag. Data are presented as means ± SEMs from 3 or more independent biological replicates.

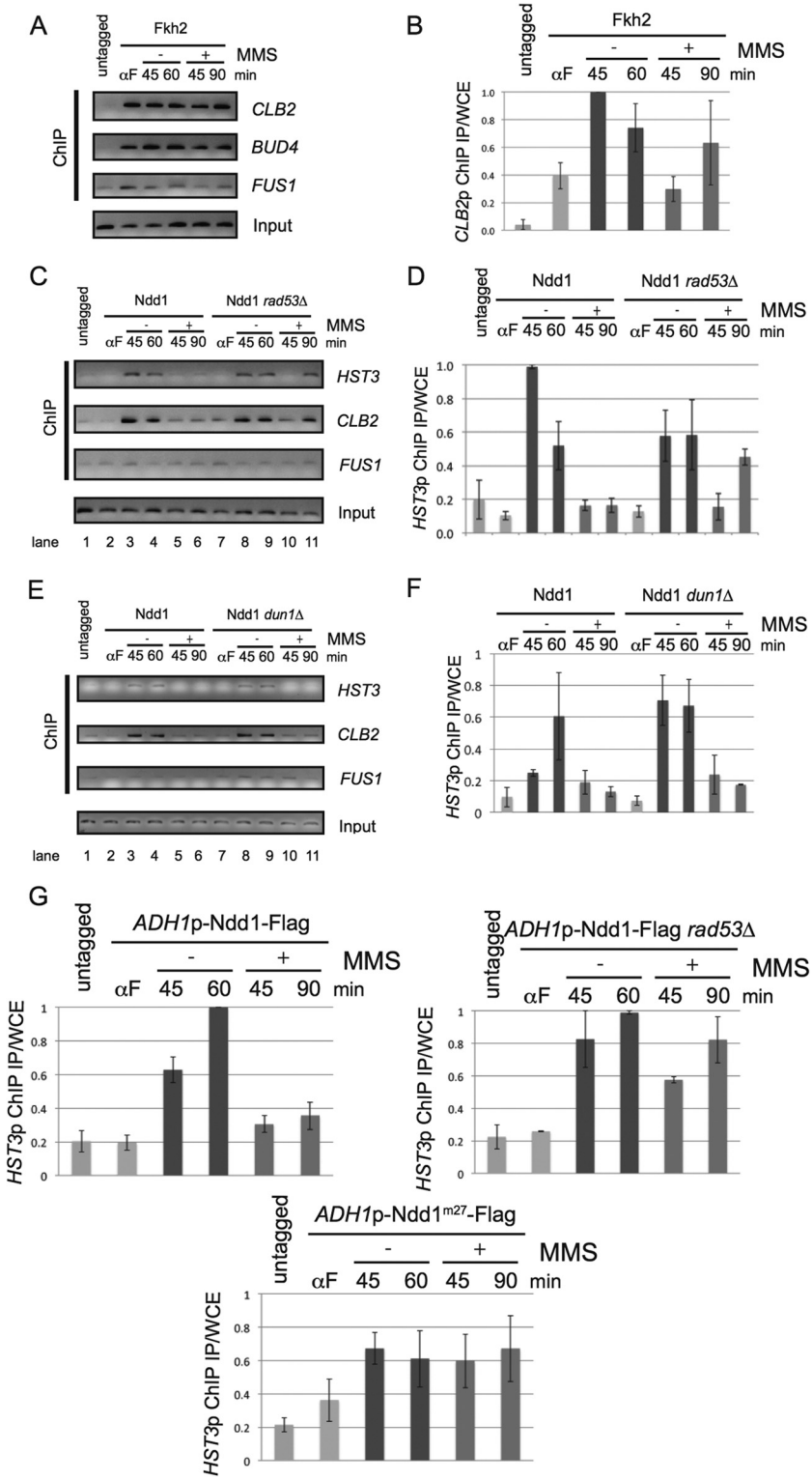

FIG 4 Rad53 phosphorylation of Ndd1 blocks its association with its target gene promoters. (A) ChIP was performed by affinity purification with an anti-Flag antibody from an untagged strain or a strain with Fkh2-Flag. Target DNA sequences were amplified by PCR. Results for two different mitotic gene promoters (*CLB2* and *BUD4*) are shown, along with those for a negative-control locus (*FUS1*). Input is shown from *CLB2* primers. The untagged control is from an asynchronous culture. For all others, cells were arrested in G_1 with α-factor and released into the absence (−) or presence (+) of 0.05% MMS for the indicated times. A small amount of background binding was observed at *FUS1*, independently of a tagged Fkh2. (B) ChIP of Fkh2-Flag quantified by qPCR of the *CLB2* promoter. The ratio of IP/WCE was taken for each sample. IP/WCE ratios were then normalized by setting the maximum ratio at 1 within each experiment. Data are shown as the means of the normalized values ± SEMs from 2 to 3 independent biological replicates. (C) ChIP was performed as described for panel A from an untagged strain or a strain with Ndd1-Flag. Results for two different mitotic gene promoters (*HST3* and *CLB2*) are shown, along with those for a

The *NDD1*^{10A} mutant, on the other hand, had higher mitotic transcription levels than the *NDD1*^{wt} strain, consistent with published observations that PKC phosphorylation on the C terminus of *NDD1* inhibits its transcriptional activity during an unperturbed cell cycle (11). Much like the *NDD1*^{wt} strain, in the *NDD1*^{10A} mutant, *HST3* transcription was repressed in response to damage, suggesting that much of the transcriptional repression of *HST3* is due to modification of the N-terminal half of *NDD1*.

Because of the different levels of mitotic transcriptional activity in each of our mutants, we measured the fold repression (calculated as the ratio of the level of mitotic transcription to the level of damaged transcription, so a value of 1 reflects equal transcription under the two conditions) using the same time points used in Fig. 2C in order to compare all our strains. We confirmed that the *NDD1*^{wt} strain and the *ndd1*^{m27} mutant are in the same cell cycle position as each other both for the mitotic time point and for the damaged time point used (see Fig. S2C and D in the supplemental material). *HST3* was 3-fold repressed in response to DNA damage in a wild-type cell, and this repression was lost in a *rad53*Δ mutant, which showed 0.6-fold repression (Fig. 2C and 3A). The *ndd1*^{m27} mutant had equal levels of transcription in the presence and absence of damage, showing approximately 1.2-fold repression ($P = 0.0013$ by one-tailed Student *t* test), and the *rad53*Δ mutant was epistatic to the *ndd1*^{m27} mutant for this (0.7-fold repressed). The *NDD1*^{10A} mutant was 2.3-fold repressed in response to damage (a result not significantly different from that for the *NDD1*^{wt} strain; $P = 0.21$ by one-tailed Student *t* test). Both the *ndd1*^{m17} and *ndd1*^{25A} mutants significantly relieved this repression, with the *ndd1*^{m17} mutant showing 1.2-fold repression ($P = 0.0089$ by one-tailed Student *t* test) and the *ndd1*^{25A} mutant showing 1.4-fold repression ($P = 0.016$ by one-tailed Student *t* test).

To determine whether these effects were generalizable to the entire *CLB2* cluster, we examined two other mitotic genes in this group using the *ndd1*^{m27} complete site mutant. The *ndd1*^{m27} mutation also significantly relieved the transcriptional repression of *CDC5* (Fig. 3B) ($P = 0.045$ by one-tailed Student *t* test) and *ALK1* (Fig. 3C) ($P = 0.0037$ by one-tailed Student *t* test). Deletion of *RAD53* led to slightly higher relative transcription in response to damage compared to that in the *ndd1*^{m27} mutants, suggesting that we missed some Rad53 phosphorylation sites or that Rad53 may have an additional target that contributes to downregulation of the *CLB2* cluster.

Rad53 blocks Ndd1 association with its target gene promoters. We next wanted to know how Rad53-dependent phosphorylation of Ndd1 affected Ndd1's function. Mcm1 and Fkh2 are present at the promoters of these mitotic genes throughout the cell cycle and coordinate both repression and activation by recruiting additional transcriptional regulators (4, 5). Ndd1 is recruited to mitotic gene promoters through a phosphorylation-dependent interaction with the forkhead-associated (FHA) domain of Fkh2 (8, 27). We used chromatin immunoprecipitation (ChIP) to examine the recruitment of Fkh2 and Ndd1 to the promoters of members of the *CLB2* cluster. Fkh2 bound to the promoters of *BUD4* and *CLB2*, two members of this cluster, throughout an undamaged cell cycle (consistent with the findings of Koranda et al. [4]) and in the presence DNA damage (Fig. 4A; quantification is provided in Fig. 4B), although some cell cycle alterations were seen. Ndd1, on the other hand, was recruited to mitotic gene promoters in an undamaged mitosis, but Ndd1 binding to its target promoters was reduced to background levels in G_1 or in response to DNA damage (Fig. 4C, lanes 2 to 6; quantification is provided in Fig. 4D). Rad53 was required for the loss of association of Ndd1 with its target promoters in response to DNA damage but not in G_1, as association of Ndd1 to its target promoters was significantly rescued by 90 min after release into MMS (Fig. 4C, lanes 7 to 11; quantification is provided in Fig. 4D) ($P = 0.0034$ by one-tailed Student *t* test comparing *RAD53* and *rad53*Δ ChIP results). This suggested that Rad53-dependent phosphorylation of Ndd1 blocked its recruitment to its target gene promoters, perhaps by blocking the interaction of Ndd1 with Fkh2. Consistent with our transcriptional data showing a checkpoint-independent delay in the cell cycle (see Fig. S2B in the supplemental material) and the accumulation of *HST3* mRNA in response to damage (Fig. 2A), Ndd1 association with its targets was also delayed in MMS-treated *rad53*Δ strains compared to that in untreated cells. This likely represents a nonspecific delay due to alkylation of the genome. Dun1 was not required to block Ndd1 binding to its target promoters in response to DNA damage (Fig. 4E; quantification is provided in Fig. 4F), suggesting, again, that Rad53 has a stronger effect than Dun1 on Ndd1 inhibition. Finally, we tested whether mutation of the Rad53-dependent sites identified on Ndd1 was sufficient to restore binding of Ndd1 to its target promoters using Flag-tagged Ndd1 under the control of the *ADH1* promoter. Ndd1^{wt} had significantly lower binding to *HST3* in response to DNA damage in *RAD53* cells (Fig. 4G) ($P = 0.008$ by one-tailed Student *t* test comparing the mitotic sample at 60 min to the damaged sample at 90 min), whereas Ndd1^{wt} binding to *HST3* was unchanged by DNA damage in a *rad53*Δ strain. In contrast, Ndd1^{m27} bound to *HST3* independently of DNA damage, even in the presence of an active checkpoint. The same pattern was seen at the *CLB2* promoter (see Fig. S3 in the supplemental material).

As an independent way to test whether Rad53 blocked the interaction between Fkh2 and Ndd1 in response to DNA damage, we used a system where *GAL1* transcription was controlled by a fusion of Fkh2 with the Gal4 DNA-binding domain ($Gal4_{DBD}$). Previous work has shown that transcription of the $Gal4_{DBD}$-Fkh2 fusion is dependent on Ndd1 (8, 27), so this system allowed us to look at the interaction between Fkh2 and Ndd1 in isolation. We arrested cells in G_1 with α-factor and released them into the cell cycle in the absence or presence of 0.05% MMS. $Gal4_{DBD}$-Fkh2-driven transcription of *GAL1* was high in an undamaged mitosis and low in G_1 phase, irrespective of *RAD53*. In contrast, Rad53 activity was required to block transcription in response to DNA damage (Fig. 5A). This correlated with the binding of Ndd1 at

negative-control locus (*FUS1*). Input from *HST3* primers is shown. (D) Ndd1-Flag ChIP was quantified by qPCR of the *HST3* promoter and normalized as described for panel B. As described for panel B, data are presented as means ± SEMs from 2 to 4 independent biological replicates. (E) ChIP was performed as described above in wild-type and *dun1*Δ strains. Input from *HST3* primers is shown. (F) Quantification was done as described for panel D from 3 independent biological replicates. (G) ChIP was performed from an untagged strain or a strain with Ndd1-Flag under the control of the *ADH1* promoter (*ADH1*p). ChIP was quantified by qPCR of the *HST3* promoter (*HST3*p) and normalized as described for panel B and panel D. Data are presented as means ± SEMs from 2 (for both *NDD1*^{wt} and *NDD1*^{wt} *rad53*Δ strains) or 4 (for the *ndd1*^{m27} mutant) independent biological replicates.

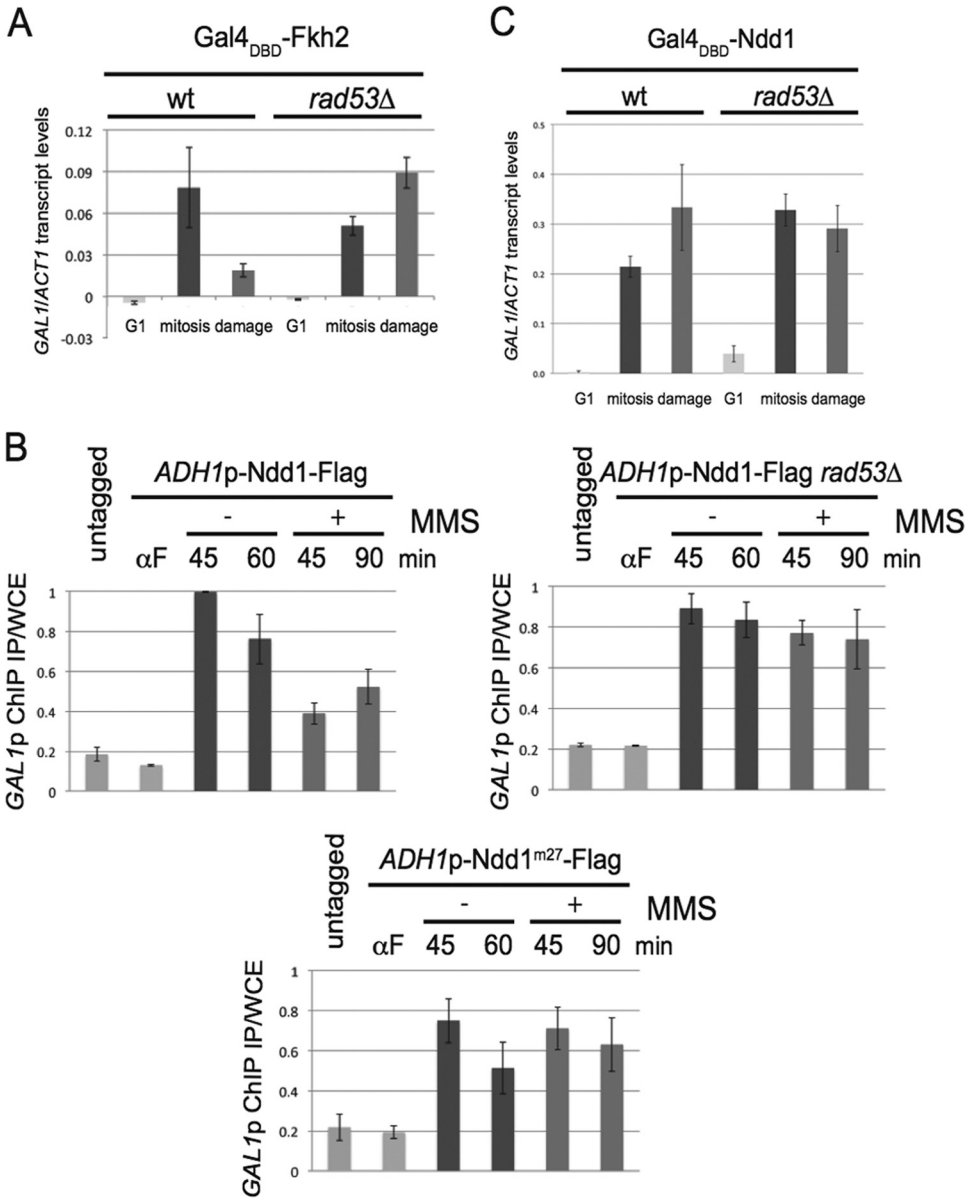

FIG 5 Rad53 does not affect the inherent transcriptional activator activity of Ndd1. (A) The Gal4 DNA-binding domain fused to Fkh2 was used to measure the transcriptional activity at the *GAL1* locus by RT-qPCR in wild-type and *rad53*Δ strains with Ndd1 under the control of the *ADH1* promoter. Cells were arrested in G_1 with α-factor and released into the absence (mitosis) or presence (damage) of MMS for 45 min or 90 min, respectively. Data are presented as *GAL1* transcript levels normalized to *ACT1* levels, with the background of a Gal4 DNA-binding domain alone subtracted from each. Data are presented as means ± SEMs from at least 3 independent biological replicates. (B) ChIP was performed by affinity purification with an anti-Flag antibody from an untagged strain or a strain with Ndd1-Flag under the control of the *ADH1* promoter in the presence of the $Gal4_{DBD}$-Fkh2 plasmid. ChIP was quantified by qPCR of the *GAL1* promoter. The ratio of IP/WCE was taken for each sample. IP/WCE ratios were then normalized by setting the maximum ratio at 1 within each experiment. Data are shown as the means of the normalized values ± SEMs from 3 (for both $NDD1^{wt}$ and $NDD1^{wt}$ *rad53*Δ strains) or 6 (for the $ndd1^{m27}$ mutant) independent biological replicates. The untagged control is from an asynchronous culture. For all others, cells were arrested in G_1 with α-factor and released into the absence (−) or presence (+) of 0.05% MMS for the indicated times. (C) The Gal4 DNA-binding domain was fused directly to Ndd1 to measure the transcriptional activator activity of Ndd1 at the endogenous *GAL1* locus by RT-qPCR, and the results were normalized as described for panel A. Cells were arrested in G_1 with α-factor and released into the absence (mitosis) or presence (damage) of MMS for 45 min. Data are presented as means ± SEMs from 4 to 6 biological replicates.

GAL1 (Fig. 5B), which was reduced in response to damage in wild-type cells but not in *rad53*Δ cells or in the $Ndd1^{m27}$ site mutant. As further confirmation, the same pattern was seen at another Gal4-regulated gene, *GAL2* (see Fig. S4 in the supplemental material). To test whether the observed Rad53-dependent transcriptional changes were due to Ndd1 recruitment, as opposed to a direct effect on Ndd1 transactivator activity itself, we fused the $Gal4_{DBD}$ directly to Ndd1 and again measured transcriptional activity at the *GAL1* locus (7–9). We arrested cells in G_1 with α-factor and released them into the cell cycle in the absence or presence of 0.05% MMS. $Gal4_{DBD}$-Ndd1 promoted transcription in mitosis but not in G_1, consistent with the observation that mutation of CDK or Polo phosphorylation sites in Ndd1 reduces its intrinsic transcriptional activator activity (7, 27). $Gal4_{DBD}$-Ndd1 drove

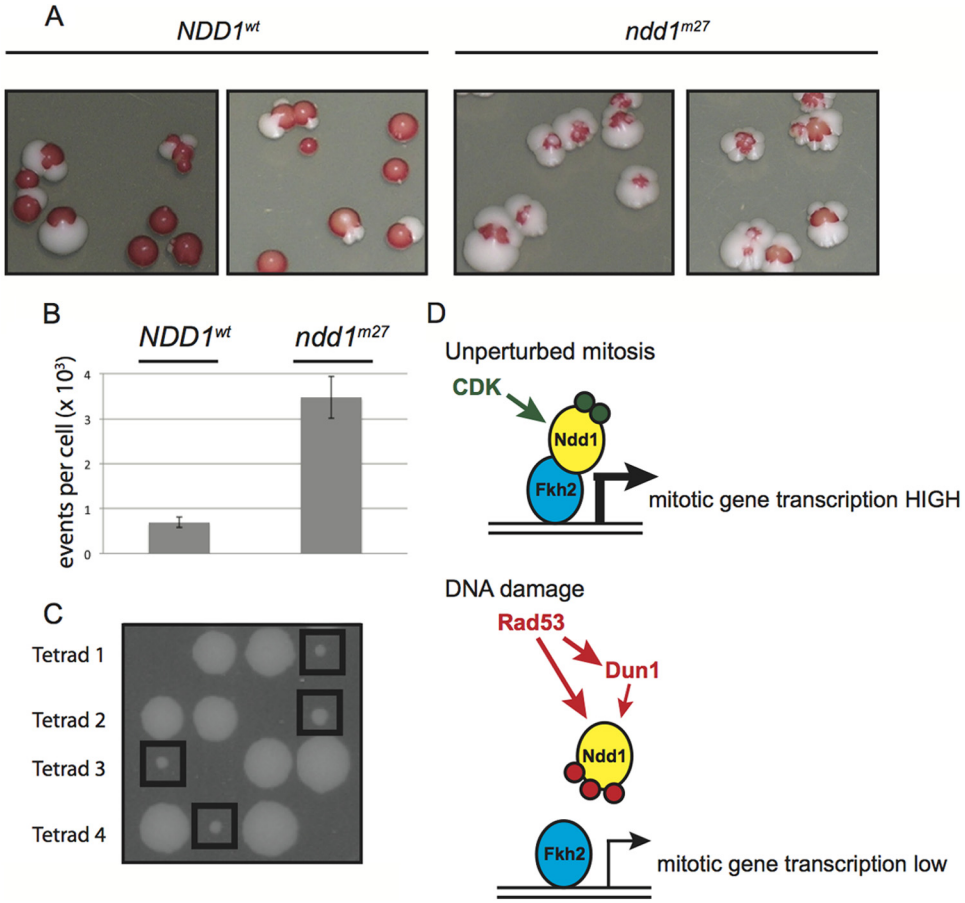

FIG 6 Downregulation of Ndd1 is important for the genome stability and viability of *rad53*Δ strains. (A) *NDD1*^{wt} *ade2 ade3* and *ndd1*^{m27} *ade2 ade3* strains with an extra chromosome VII (containing *CYH2* and *ADE3*) were grown on a nonselective plate and photographed. White sectors in otherwise red colonies suggest chromosome loss. (B) Chromosome loss events were quantified by determining the number of cycloheximide-resistant, white colony-forming cells in a population. Data are presented as means ± SEMs from 17 (the *NDD1*^{wt} strain) or 19 (*ndd1*^{m27} mutant) biological replicates. (C) *ndd1*^{hyp} rescues the lethality of *rad53*Δ. Results for four tetratype tetrads are shown. Black boxes are around *ndd1*^{hyp} *rad53*Δ spores. The single dead spore within each tetrad is inferred to be *NDD1*^{wt} *rad53*Δ. Both *NDD1*^{wt} and *ndd1*^{hyp} spores are healthy in the absence of *rad53*Δ. (D) During an unperturbed mitosis, Ndd1 associates with Fkh2 to drive high levels of mitotic gene transcription, an interaction that is promoted by CDK phosphorylation. In response to DNA damage, Rad53 activation leads to Ndd1 phosphorylation both directly and through the activation of Dun1. Rad53-dependent phosphorylation of Ndd1 blocks its association with Fkh2, keeping mitotic gene transcription low.

high levels of transcription independently of DNA damage and *RAD53* status (Fig. 5C). Together, these data support a model in which Rad53's function is exclusively to block Ndd1's interaction with Fkh2. This is in contrast to the cell cycle-regulated phosphorylation of Ndd1, which affects both its interaction with Fkh2 and its intrinsic transactivator function.

Ndd1 downregulation is an essential function of Rad53. Finally, we wanted to know the consequence of failing to repress mitotic gene transcription. We tested whether mutation of the 27 Rad53-dependent sites on Ndd1 affected spontaneous chromosome loss rates by measuring the frequency of spontaneous chromosome loss in strains carrying an extra copy of chromosome VII (29, 30). The fact that *RAD53* is essential, even in the absence of exogenous DNA-damaging agents, suggests that it is active during an unperturbed cell cycle to respond to low levels of damage that arise even in an unperturbed S phase. In this strain, chromosome loss can be seen either by the generation of cycloheximide-resistant colonies or by the appearance of white sectors in the otherwise red colonies. As shown in Fig. 6A, we saw an increase in white sectoring in the *ndd1*^{m27} strain relative to that in the wild type, suggesting that this mutant has a higher rate of spontaneous chromosome loss. We quantified the frequency of chromosome loss by counting white, cycloheximide-resistant colonies and observed a 5-fold higher level in *ndd1*^{m27} mutants than in *NDD1* cells (Fig. 6B) ($P < 0.001$ by two-tailed Student *t* test). This suggests that proper regulation of Ndd1 is an important function of Rad53; however, the interpretation of this experiment is slightly complicated since the *ndd1*^{m27} mutant had lower peak transcriptional activity than wild-type *NDD1*. To test whether the chromosome loss phenotype of the *ndd1*^{m27} mutant was associated with the gain-of-function ability of the *ndd1*^{m27} allele to be refractory to Rad53 inhibition, we repeated the chromosome loss assay with a copy of *ndd1*^{m27} in the presence of *NDD1*^{wt}. As shown in Fig. S5A in the supplemental material, an additional copy of *ndd1*^{m27} was sufficient to increase the chromosome loss frequency by 2.6-fold ($P < 0.001$ by two-tailed Student *t* test). In addition, *ndd1*^{m17} and *ndd1*^{25A}, which similarly blocked transcriptional repression in response to DNA damage, also significantly increased the chromo-

some loss frequency when expressed in the presence of *NDD1*^{wt} (a 2-fold increase for *ndd1*^{m17} and a 1.6-fold increase for *ndd1*^{25A}; $P = 0.008$ and 0.025, respectively, by two-tailed Student *t* test). Moreover, *ndd1*^{m27}, the most hypomorphic, showed the strongest dominant effect, whereas the less hypomorphic alleles showed a reduced dominant effect.

As an independent way to evaluate the significance of Ndd1 inhibition by Rad53, we tested if downregulation of Ndd1 was an essential function of Rad53. *RAD53* is an essential gene. Previously, Sml1 downregulation by Rad53 (via Dun1) was shown to be an important function of Rad53 because *sml1*Δ rescues the lethality of *RAD53* deletion (31). Because *NDD1* is itself essential, we generated a hypomorphic *ndd1*^{hyp} allele by mutating a subset of its CDK phosphorylation sites (27), leaving intact all of the Rad53-dependent phosphorylation sites (see Materials and Methods for details). The *ndd1*^{hyp} mutant showed no fitness defect, yet *ndd1*^{hyp} rescued the viability of the *rad53*Δ mutant (Fig. 6C). The effect was 83% penetrant, as 29 out of 35 spores whose genotype could be unambiguously identified as *ndd1*^{hyp} *rad53*Δ were viable. As with *sml1*Δ *rad53*Δ cells, *ndd1*^{hyp} *rad53*Δ double mutants grew more slowly than *RAD53* cells. However, higher levels of bypass suppression might be seen with other *NDD1* alleles. Furthermore, *ndd1*^{hyp} *rad53*Δ *sml1*Δ cells were slightly less sensitive to growth in the presence of MMS than *NDD1*^{wt} *rad53*Δ *sml1*Δ cells (see Fig. S5B in the supplemental material), further highlighting the importance of the downregulation of Ndd1 for the checkpoint response.

DISCUSSION

Genes whose functions are required uniquely in mitosis have evolved to contain similar promoters, such that the expression of each can be controlled by a common set of cell cycle-regulated transcription factors. We have found that upon DNA damage, it is advantageous for the cell to limit the expression of this cluster (see also the accompanying paper [33]). We show that this is achieved by inactivation of the Ndd1 transcription factor primarily by Rad53 but also by Dun1, leading to the transcriptional downregulation of the *CLB2* cluster (Fig. 6D), though we have been unable to show direct phosphorylation of Ndd1 by either kinase, and therefore it remains a formal possibility that the *DUN1/RAD53* dependence of these phosphorylations is indirect. As the manuscript was being prepared, the findings of a study that looked globally at changes to transcription factors in response to DNA damage were published (32). In further support of our model, this study (32) shows that transcription of the entire *CLB2* cluster is downregulated in response to DNA damage and that the downregulation is fully dependent on *RAD53* and partially dependent on *DUN1*.

A key characteristic of the transcriptional response of the *CLB2* cluster is that it is incomplete (Fig. 2Ai). Transcription in the presence of DNA damage is still severalfold higher than that in G_1-arrested cells. During the normal transition from G_1 to mitosis, two things happen: the histone deacetylase complex Sin3-Rpd3, which actively represses transcription in G_1, is removed (26), and Ndd1 is recruited to induce transcriptional activation (4, 7–9, 27). Previous work has shown that the Sin3-Rpd3 complex is released from *CLB2* cluster promoters when cells exit G_1 even in the absence of Ndd1 (26). Therefore, we hypothesize that the transcriptional repression of the cluster is still released but that the DNA damage checkpoint inhibits transcriptional activation of the cluster by inactivating Ndd1, leading to the observed partial transcriptional downregulation.

Previous work has shown that though all members of the *CLB2* cluster are downregulated transcriptionally (1), the levels of the corresponding proteins vary following treatment with DNA damage agents (2). For example, Clb2 eventually accumulates to very high levels in response to DNA damage (2), and the cyclin-CDK function is important for the activity of the checkpoint itself (2, 34–38). Why turn down the *CLB2* cluster when the maintenance of Clb2 levels is important? Perhaps this reflects the evolution of the system to respond differently to different degrees of stress. In *Escherichia coli*, low levels of stress stimulate only a subset of the SOS response target genes. Increasing stress leads to more target genes being turned on (39). A similar principle may be at work in eukaryotes, with graded responses needed with different amounts of damage. In the presence of DNA damage that can be quickly repaired, decreasing the levels of mitotic drivers, such as Clb2 and the Polo kinase Cdc5, might help the cell acutely slow mitosis. The extended metaphase arrest necessary in the presence of prolonged damage may require high Clb2 levels. A fine-tuning of this system may be especially important for Cdc5, which is a critical regulator of adaptation to irreparable damage (40) and must eventually accumulate to high levels to inactivate Rad53 and the checkpoint after several hours (41, 42). The transcriptional downregulation of Cdc5 may keep it from accumulating too quickly and prematurely inactivating the checkpoint.

In mammals, the FoxM1-regulated cluster includes G_2 genes, such as Plk1 and cyclin B (43), and FoxM1 is downregulated in response to DNA damage (44). The lab of R. H. Medema recently showed that there is still transcription of this cluster and that the residual transcription is important for the cell's capacity to recover following repair of DNA damage (45). This may be another aspect of the incomplete transcriptional response observed with the *CLB2* cluster: it allows some mitotic regulators to be present, such that when the damage has been repaired, the cell is poised for mitosis.

Here, we describe how Rad53-dependent phosphorylation inactivates Ndd1 by preventing its recruitment to its target genes by blocking its interaction with its binding partner, Fkh2. This mechanism is reminiscent of inhibition of other proteins, such as Sld3 and Nrm1, whose phosphorylation by Rad53 disrupts their interactions with their normal binding partners (20, 21, 46, 47). For both Ndd1 and Fkh2 as well as Sld3 and its binding partner, Dpb11, Rad53 acts by disrupting an existing phosphorylation-dependent interaction promoted by CDK (6, 8, 27, 48).

Recent work suggests that protein kinase C (PKC) inhibits Ndd1 during S phase (11). We found one of the two identified PKC sites in our purifications to be a Rad53-dependent phosphorylation site, which was mutated in our *ndd1*^{m27} allele. In addition to phosphorylating Ndd1 directly, Rad53 may also promote PKC activity in response to damage. More likely, the very C terminus of Ndd1 (which contains 6 of our 27 mutated sites and both PKC sites identified) might be accessible for modification by different kinases under different circumstances. Our analysis of two different subsets of phosphorylation sites on Ndd1 (*ndd1*^{10A} and *ndd1*^{m17}) suggests that the phosphorylation sites critical for inhibiting Ndd1 in response to DNA damage are in the N-terminal half of the protein and, therefore, are independent of PKC.

Transcriptional regulation of gene clusters in response to DNA damage is a common theme (1). For many of these clusters, the

transcription factors targeted by the checkpoint machinery and the molecular mechanisms of the response have still not been worked out, although recent work has begun this effort (32). The regulation of these clusters is likely to be critical to the cell's ability to properly respond to DNA damage.

ACKNOWLEDGMENTS

We thank D. Durocher for DAB001. We also thank C. Gross, H. Madhani, P. O'Farrell, and members of the D. P. Toczyski lab for helpful discussions and I. Foe for critical reading of the manuscript.

This work was supported by the National Science Foundation under grant no. 1144247 (to E.R.E.), National Institutes of Health grants GM059691 (to D.P.T.), GM089778 (to J.W.), and R00GM085013 (to J.A.B.), and funds from the Jonsson Cancer Center at UCLA (to J.W.).

REFERENCES

1. **Gasch AP, Huang M, Metzner S, Botstein D, Elledge SJ, Brown PO.** 2001. Genomic expression responses to DNA-damaging agents and the regulatory role of the yeast ATR homolog Mec1p. Mol. Biol. Cell **12:**2987–3003. http://dx.doi.org/10.1091/mbc.12.10.2987.
2. **Maas NL, Miller KM, DeFazio LG, Toczyski DP.** 2006. Cell cycle and checkpoint regulation of histone H3 K56 acetylation by Hst3 and Hst4. Mol. Cell **23:**109–119. http://dx.doi.org/10.1016/j.molcel.2006.06.006.
3. **Spellman PT, Sherlock G, Zhang MQ, Iyer VR, Anders K, Eisen MB, Brown PO, Botstein D, Futcher B.** 1998. Comprehensive identification of cell cycle-regulated genes of the yeast Saccharomyces cerevisiae by microarray hybridization. Mol. Biol. Cell **9:**3273–3297. http://dx.doi.org/10.1091/mbc.9.12.3273.
4. **Koranda M, Schleiffer A, Endler L, Ammerer G.** 2000. Forkhead-like transcription factors recruit Ndd1 to the chromatin of G_2/M-specific promoters. Nature **406:**94–98. http://dx.doi.org/10.1038/35017589.
5. **Zhu G, Spellman PT, Volpe T, Brown PO, Botstein D, Davis TN, Futcher B.** 2000. Two yeast forkhead genes regulate the cell cycle and pseudohyphal growth. Nature **406:**90–94. http://dx.doi.org/10.1038/35017581.
6. **Pic-Taylor A, Darieva Z, Morgan BA, Sharrocks AD.** 2004. Regulation of cell cycle-specific gene expression through cyclin-dependent kinase-mediated phosphorylation of the forkhead transcription factor Fkh2p. Mol. Cell. Biol. **24:**10036–10046. http://dx.doi.org/10.1128/MCB.24.22.10036-10046.2004.
7. **Darieva Z, Bulmer R, Pic-Taylor A, Doris KS, Geymonat M, Sedgwick SG, Morgan BA, Sharrocks AD.** 2006. Polo kinase controls cell-cycle-dependent transcription by targeting a coactivator protein. Nature **444:**494–498. http://dx.doi.org/10.1038/nature05339.
8. **Darieva Z, Pic-Taylor A, Boros J, Spanos A, Geymonat M, Reece RJ, Sedgwick SG, Sharrocks AD, Morgan BA.** 2003. Cell cycle-regulated transcription through the FHA domain of Fkh2p and the coactivator Ndd1p. Curr. Biol. **13:**1740–1745. http://dx.doi.org/10.1016/j.cub.2003.08.053.
9. **Loy CJ, Lydall D, Surana U.** 1999. NDD1, a high-dosage suppressor of cdc28-1N, is essential for expression of a subset of late-S-phase-specific genes in Saccharomyces cerevisiae. Mol. Cell. Biol. **19:**3312–3327.
10. **Pramila T, Wu W, Miles S, Noble WS, Breeden LL.** 2006. The Forkhead transcription factor Hcm1 regulates chromosome segregation genes and fills the S-phase gap in the transcriptional circuitry of the cell cycle. Genes Dev. **20:**2266–2278. http://dx.doi.org/10.1101/gad.1450606.
11. **Darieva Z, Han N, Warwood S, Doris KS, Morgan BA, Sharrocks AD.** 2012. Protein kinase C regulates late cell cycle-dependent gene expression. Mol. Cell. Biol. **32:**4651–4661. http://dx.doi.org/10.1128/MCB.06000-11.
12. **Pramila T, Miles S, GuhaThakurta D, Jemiolo D, Breeden LL.** 2002. Conserved homeodomain proteins interact with MADS box protein Mcm1 to restrict ECB-dependent transcription to the M/G_1 phase of the cell cycle. Genes Dev. **16:**3034–3045. http://dx.doi.org/10.1101/gad.1034302.
13. **Darieva Z, Clancy A, Bulmer R, Williams E, Pic-Taylor A, Morgan BA, Sharrocks AD.** 2010. A competitive transcription factor binding mechanism determines the timing of late cell cycle-dependent gene expression. Mol. Cell **38:**29–40. http://dx.doi.org/10.1016/j.molcel.2010.02.030.
14. **Segurado M, Tercero JA.** 2009. The S-phase checkpoint: targeting the replication fork. Biol. Cell **101:**617–627. http://dx.doi.org/10.1042/BC20090053.
15. **Longhese MP, Foiani M, Muzi-Falconi M, Lucchini G, Plevani P.** 1998. DNA damage checkpoint in budding yeast. EMBO J. **17:**5525–5528. http://dx.doi.org/10.1093/emboj/17.19.5525.
16. **Melo J, Toczyski D.** 2002. A unified view of the DNA-damage checkpoint. Curr. Opin. Cell Biol. **14:**237–245. http://dx.doi.org/10.1016/S0955-0674(02)00312-5.
17. **Sanchez Y, Bachant J, Wang H, Hu F, Liu D, Tetzlaff M, Elledge SJ.** 1999. Control of the DNA damage checkpoint by Chk1 and Rad53 protein kinases through distinct mechanisms. Science **286:**1166–1171. http://dx.doi.org/10.1126/science.286.5442.1166.
18. **Wang H, Liu D, Wang Y, Qin J, Elledge SJ.** 2001. Pds1 phosphorylation in response to DNA damage is essential for its DNA damage checkpoint function. Genes Dev. **15:**1361–1372. http://dx.doi.org/10.1101/gad.893201.
19. **Agarwal R, Tang Z, Yu H, Cohen-Fix O.** 2003. Two distinct pathways for inhibiting pds1 ubiquitination in response to DNA damage. J. Biol. Chem. **278:**45027–45033. http://dx.doi.org/10.1074/jbc.M306783200.
20. **Lopez-Mosqueda J, Maas NL, Jonsson ZO, Defazio-Eli LG, Wohlschlegel J, Toczyski DP.** 2010. Damage-induced phosphorylation of Sld3 is important to block late origin firing. Nature **467:**479–483. http://dx.doi.org/10.1038/nature09377.
21. **Zegerman P, Diffley JF.** 2010. Checkpoint-dependent inhibition of DNA replication initiation by Sld3 and Dbf4 phosphorylation. Nature **467:**474–478. http://dx.doi.org/10.1038/nature09373.
22. **Allen JB, Zhou Z, Siede W, Friedberg EC, Elledge SJ.** 1994. The SAD1/RAD53 protein kinase controls multiple checkpoints and DNA damage-induced transcription in yeast. Genes Dev. **8:**2401–2415. http://dx.doi.org/10.1101/gad.8.20.2401.
23. **Elledge SJ.** 1996. Cell cycle checkpoints: preventing an identity crisis. Science **274:**1664–1672. http://dx.doi.org/10.1126/science.274.5293.1664.
24. **Weinert T, Little E, Shanks L, Admire A, Gardner R, Putnam C, Michelson R, Nyberg K, Sundareshan P.** 2000. Details and concerns regarding the G_2/M DNA damage checkpoint in budding yeast. Cold Spring Harbor Symp. Quant. Biol. **65:**433–442. http://dx.doi.org/10.1101/sqb.2000.65.433.
25. **Sidorova JM, Breeden LL.** 1997. Rad53-dependent phosphorylation of Swi6 and down-regulation of CLN1 and CLN2 transcription occur in response to DNA damage in Saccharomyces cerevisiae. Genes Dev. **11:**3032–3045. http://dx.doi.org/10.1101/gad.11.22.3032.
26. **Veis J, Klug H, Koranda M, Ammerer G.** 2007. Activation of the G_2/M-specific gene CLB2 requires multiple cell cycle signals. Mol. Cell. Biol. **27:**8364–8373. http://dx.doi.org/10.1128/MCB.01253-07.
27. **Reynolds D, Shi BJ, McLean C, Katsis F, Kemp B, Dalton S.** 2003. Recruitment of Thr 319-phosphorylated Ndd1p to the FHA domain of Fkh2p requires Clb kinase activity: a mechanism for CLB cluster gene activation. Genes Dev. **17:**1789–1802. http://dx.doi.org/10.1101/gad.1074103.
28. **Hartwell LH.** 1967. Macromolecule synthesis in temperature-sensitive mutants of yeast. J. Bacteriol. **93:**1662–1670.
29. **Galgoczy DJ, Toczyski DP.** 2001. Checkpoint adaptation precedes spontaneous and damage-induced genomic instability in yeast. Mol. Cell. Biol. **21:**1710–1718. http://dx.doi.org/10.1128/MCB.21.5.1710-1718.2001.
30. **Sandell LL, Zakian VA.** 1993. Loss of a yeast telomere: arrest, recovery, and chromosome loss. Cell **75:**729–739. http://dx.doi.org/10.1016/0092-8674(93)90493-A.
31. **Zhao X, Muller EG, Rothstein R.** 1998. A suppressor of two essential checkpoint genes identifies a novel protein that negatively affects dNTP pools. Mol. Cell **2:**329–340. http://dx.doi.org/10.1016/S1097-2765(00)80277-4.
32. **Jaehnig EJ, Kuo D, Hombauer H, Ideker TG, Kolodner RD.** 2013. Checkpoint kinases regulate a global network of transcription factors in response to DNA damage. Cell Rep. **4:**174–188. http://dx.doi.org/10.1016/j.celrep.2013.05.041.
33. **Yelamanchi SK, Veis J, Anrather D, Klug H, Ammerer G.** 2014. Genotoxic stress prevents Ndd1-dependent transcriptional activation of G_2/M-specific genes in *Saccharomyces cerevisiae*. Mol. Cell. Biol. **34:**711–724. http://dx.doi.org/10.1128/MCB.01090-13.
34. **Bonilla CY, Melo JA, Toczyski DP.** 2008. Colocalization of sensors is sufficient to activate the DNA damage checkpoint in the absence of damage. Mol. Cell **30:**267–276. http://dx.doi.org/10.1016/j.molcel.2008.03.023.
35. **Du LL, Nakamura TM, Russell P.** 2006. Histone modification-dependent and -independent pathways for recruitment of checkpoint protein Crb2 to double-strand breaks. Genes Dev. **20:**1583–1596. http://dx.doi.org/10.1101/gad.1422606.

36. **Pfander B, Diffley JF.** 2011. Dpb11 coordinates Mec1 kinase activation with cell cycle-regulated Rad9 recruitment. EMBO J. **30:**4897–4907. http://dx.doi.org/10.1038/emboj.2011.345.
37. **Ira G, Pellicioli A, Balija A, Wang X, Fiorani S, Carotenuto W, Liberi G, Bressan D, Wan L, Hollingsworth NM, Haber JE, Foiani M.** 2004. DNA end resection, homologous recombination, and DNA damage checkpoint activation require CDK1. Nature **431:**1011–1017. http://dx.doi.org/10.1038/nature02964.
38. **Clerici M, Baldo V, Mantiero D, Lottersberger F, Lucchini G, Longhese MP.** 2004. A Tel1/MRX-dependent checkpoint inhibits the metaphase-to-anaphase transition after UV irradiation in the absence of Mec1. Mol. Cell. Biol. **24:**10126–10144. http://dx.doi.org/10.1128/MCB.24.23.10126-10144.2004.
39. **Sutton MD, Smith BT, Godoy VG, Walker GC.** 2000. The SOS response: recent insights into umuDC-dependent mutagenesis and DNA damage tolerance. Annu. Rev. Genet. **34:**479–497. http://dx.doi.org/10.1146/annurev.genet.34.1.479.
40. **Toczyski DP, Galgoczy DJ, Hartwell LH.** 1997. CDC5 and CKII control adaptation to the yeast DNA damage checkpoint. Cell **90:**1097–1106. http://dx.doi.org/10.1016/S0092-8674(00)80375-X.
41. **Vidanes GM, Sweeney FD, Galicia S, Cheung S, Doyle JP, Durocher D, Toczyski DP.** 2010. cdc5 inhibits the hyperphosphorylation of the checkpoint kinase Rad53, leading to checkpoint adaptation. PLoS Biol. **8:**e1000286. http://dx.doi.org/10.1371/journal.pbio.1000286.
42. **Donnianni RA, Ferrari M, Lazzaro F, Clerici M, Nachimuthu BT, Plevani P, Muzi-Falconi M, Pellicioli A.** 2010. Elevated levels of the Polo kinase Cdc5 override the Mec1/ATR checkpoint in budding yeast by acting at different steps of the signaling pathway. PLoS Genet. **6:**e1000763. http://dx.doi.org/10.1371/journal.pgen.1000763.
43. **Laoukili J, Kooistra MRH, Brás A, Kauw J, Kerkhoven RM, Morrison A, Clevers H, Medema RH.** 2005. FoxM1 is required for execution of the mitotic programme and chromosome stability. Nat. Cell Biol. **7:**126–136. http://dx.doi.org/10.1038/ncb1217.
44. **Barsotti AM, Prives C.** 2009. Pro-proliferative FoxM1 is a target of p53-mediated repression. Oncogene **28:**4295–4305. http://dx.doi.org/10.1038/onc.2009.282.
45. **Alvarez-Fernandez M, Halim VA, Krenning L, Aprelia M, Mohammed S, Heck AJ, Medema RH.** 2010. Recovery from a DNA-damage-induced G_2 arrest requires Cdk-dependent activation of FoxM1. EMBO Rep. **11:**452–458. http://dx.doi.org/10.1038/embor.2010.46.
46. **Bastos de Oliveira FM, Harris MR, Brazauskas P, de Bruin RAM, Smolka MB.** 2012. Linking DNA replication checkpoint to MBF cell-cycle transcription reveals a distinct class of G_1/S genes. EMBO J. **31:**1798–1810. http://dx.doi.org/10.1038/emboj.2012.27.
47. **Travesa A, Kuo D, de Bruin RAM, Kalashnikova TI, Guaderrama M, Thai K, Aslanian A, Smolka MB, Yates JR, Ideker T, Wittenberg C.** 2012. DNA replication stress differentially regulates G_1/S genes via Rad53-dependent inactivation of Nrm1. EMBO J. **31:**1811–1822. http://dx.doi.org/10.1038/emboj.2012.28.
48. **Zegerman P, Diffley JF.** 2007. Phosphorylation of Sld2 and Sld3 by cyclin-dependent kinases promotes DNA replication in budding yeast. Nature **445:**281–285. http://dx.doi.org/10.1038/nature05432.